12-3-2013

Repeated elevational transitions in hemoglobin function during the evolution of Andean hummingbirds

Joana Projecto-Garcia
University of Nebraska–Lincoln, jucpgarcia@gmail.com

Chandrasekhar Natarajan
University of Nebraska-Lincoln, chandrasekhar.natarajan@unl.edu

Hideaki Moriyama
University of Nebraska - Lincoln, hmoriyama2@unl.edu

Roy E. Weber
Aarhus University, roy.weber@biology.au.dk

Angela Fago
Aarhus University, Denmark, angela.fago@biology.au.dk

See next page for additional authors

Repeated elevational transitions in hemoglobin function during the evolution of Andean hummingbirds

Joana Projecto-Garcia[a,1], Chandrasekhar Natarajan[a,1], Hideaki Moriyama[a], Roy E. Weber[b], Angela Fago[b], Zachary A. Cheviron[a,c], Robert Dudley[d], Jimmy A. McGuire[d,e], Christopher C. Witt[f,g,2], and Jay F. Storz[a,2,3]

[a]School of Biological Sciences, University of Nebraska, Lincoln, NE 68588; [b]Department of Bioscience, Zoophysiology, Aarhus University, DK-8000 Aarhus, Denmark; [c]Department of Animal Biology, School of Integrative Biology, University of Illinois at Urbana–Champaign, Champaign, IL 61801; [d]Department of Integrative Biology, University of California, Berkeley, CA 94720-3140; [e]Museum of Vertebrate Zoology, University of California, Berkeley, CA 94720-3160; and [f]Department of Biology and [g]Museum of Southwestern Biology, University of New Mexico, Albuquerque, NM 87131

Edited by David M. Hillis, University of Texas at Austin, Austin, TX, and approved November 8, 2013 (received for review August 15, 2013)

Animals that sustain high levels of aerobic activity under hypoxic conditions (e.g., birds that fly at high altitude) face the physiological challenge of jointly optimizing blood-O_2 affinity for O_2 loading in the pulmonary circulation and O_2 unloading in the systemic circulation. At high altitude, this challenge is especially acute for small endotherms like hummingbirds that have exceedingly high mass-specific metabolic rates. Here we report an experimental analysis of hemoglobin (Hb) function in South American hummingbirds that revealed a positive correlation between Hb-O_2 affinity and native elevation. Protein engineering experiments and ancestral-state reconstructions revealed that this correlation is attributable to derived increases in Hb-O_2 affinity in highland lineages, as well as derived reductions in Hb-O_2 affinity in lowland lineages. Site-directed mutagenesis experiments demonstrated that repeated evolutionary transitions in biochemical phenotype are mainly attributable to repeated amino acid replacements at two epistatically interacting sites that alter the allosteric regulation of Hb-O_2 affinity. These results demonstrate that repeated changes in biochemical phenotype involve parallelism at the molecular level, and that mutations with indirect, second-order effects on Hb allostery play key roles in biochemical adaptation.

high-altitude adaptation | hypoxia | parallel evolution | protein evolution | epistasis

In air-breathing vertebrates, the optimal Hb-O_2 affinity varies according to the partial pressure of atmospheric O_2 (PO_2) because of the trade-off between the need to maximize arterial O_2 saturation under hypoxia while simultaneously ensuring adequate O_2 unloading in the tissue capillaries (1–8). However, in species that are native to high-altitude environments, it is not known how often and to what extent physiological adaptation to hypoxia is mediated by genetically based modifications of Hb-O_2 affinity (9). Such questions can be resolved by conducting systematic comparative studies of Hb function among species with known phylogenetic relationships and contrasting altitudinal distributions.

In cases where multiple species have adapted independently to high-altitude hypoxia, replicated changes in Hb function may be instructive about the relative accessibility of different design solutions to natural selection. If repeated changes in Hb-O_2 affinity involve parallel amino acid substitutions, then this suggests that adaptive protein evolution may be predisposed to follow particular mutational pathways. If, by contrast, myriad different mutational changes can produce the same functional outcome, then particular design solutions may be selectively accessible from a diverse range of ancestral starting points, and pathways of protein evolution may be highly idiosyncratic.

Among vertebrates, hummingbirds have some of the highest basal metabolic rates and the highest metabolic scopes for activity, and are therefore especially compelling subjects for studies of Hb function and blood-O_2 transport under hypoxia (10–13). We conducted an experimental analysis of Hb function in 10 species of Andean hummingbirds that have dramatically different altitudinal distributions. The species included in this study fall into three main clades: the Coquettes, the Brilliants, and the Emeralds + Giant Hummingbird (*Patagona gigas*) (Fig. 1*A*). Each of these three clades contains species that are restricted to low or moderate elevations, as well as independently derived high-elevation species that routinely occur at elevations >4,200 m. We also collected data for one outgroup species from the hermit subfamily (Phaethornithinae), a primarily lowland clade that represents the likely ancestral elevational distribution for hummingbirds (14).

Results and Discussion

Hb Isoform Composition. The Hbs of birds and other jawed vertebrates are heterotetramers, composed of two α-chain and two β-chain subunits (15, 16). During postnatal life, most bird species express two main Hb isoforms in circulating red blood cells: a major isoform, HbA ($\alpha^A{}_2\beta_2$), with α-chain subunits encoded by the α^A-globin gene, and a minor isoform, HbD ($\alpha^D{}_2\beta_2$), with α-chain subunits encoded by the α^D-globin gene (17) (Fig. S1). Given that avian HbD has a consistently higher O_2-affinity relative to HbA (17), changes in the intracellular HbA/HbD ratio

Significance

Hummingbirds have exceedingly high oxygen demands because of their elevated rates of aerobic metabolism, and yet they thrive in high-altitude environments in the Andes where oxygen is scarce. Here we report the finding that when hummingbird species colonized new elevational zones, evolutionary changes in the respiratory properties of hemoglobin were repeatedly mediated by the same amino acid replacements. Specifically, ancestral sequence reconstruction and protein engineering experiments revealed that parallel adaptation of hemoglobin function in multiple species is attributable to repeated amino acid replacements at a single pair of interacting sites. This striking parallelism at the molecular level suggests a surprising degree of reproducibility and predictability in adaptive protein evolution.

Author contributions: C.C.W. and J.F.S. designed research; J.P.-G., C.N., H.M., Z.A.C., and C.C.W. performed research; H.M., R.E.W., A.F., J.A.M., C.C.W., and J.F.S. contributed new reagents/analytic tools; J.P.-G., H.M., R.E.W., A.F., Z.A.C., R.D., J.A.M., C.C.W., and J.F.S. analyzed data; and C.C.W. and J.F.S. wrote the paper.

The authors declare no conflict of interest.

This article is a PNAS Direct Submission.

Data deposition: Complete information for all specimens used in this study is archived on the ARCTOS online database (Table S4). The sequences reported in this paper have been deposited in the GenBank database (accession nos. KF222496, KF222499, KF222501, KF222503, KF222506, KF222510–KF222539).

[1]J.P.-G. and C.N. contributed equally to this work.

[2]C.C.W. and J.F.S. contributed equally to this work.

[3]To whom correspondence should be addressed. E-mail: jstorz2@unl.edu.

This article contains supporting information online at www.pnas.org/lookup/suppl/doi:10.1073/pnas.1315456110/-/DCSupplemental.

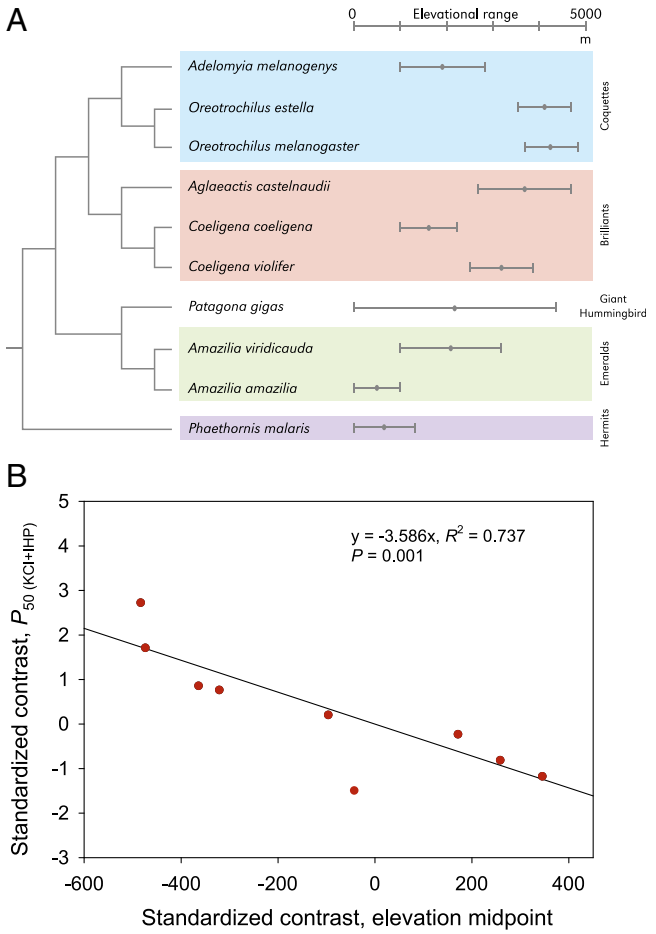

Fig. 1. Phylogenetically independent contrasts reveal a positive association between Hb-O_2 affinity and native elevation in Andean hummingbirds. (*A*) Phylogenetic relationships (25) and elevational distributions (ranges and midpoints) of 10 hummingbird species included in the analysis of Hb function. (*B*) Least-squares regression of phylogenetically independent contrasts revealed a significant negative relationship between $P_{50(KCl+IHP)}$ and native elevation (i.e., a positive relationship between Hb-O_2 affinity and elevation). See Table S2 for full results.

could substantially alter blood-O_2 affinity, and it has been suggested that regulatory changes in Hb isoform composition may contribute to adaptive changes in blood-O_2 transport in high-altitude species (18–20). To test this hypothesis we conducted a proteomic analysis of red cell lysates from each of the 10 hummingbird study species. Results of this analysis revealed that each of the hummingbird species express both HbA and HbD isoforms, and the relative concentration of the minor HbD isoform ranged from 1.6 to 24.2% (mean ± SD = 13.3 ± 6.2%). However, phylogenetically independent contrasts revealed no clear association between HbA/HbD isoform ratio and native elevation ($R^2 = 0.026$, $P = 0.657$).

Altitudinal Variation in Hb-O_2 Affinity. Evolutionary adjustments in Hb-O_2 affinity can be achieved via changes in intrinsic O_2 affinity or changes in the sensitivity of Hb to the modulating effects of physiological allosteric cofactors, such as Cl^- ions and organic phosphates (8, 15). The allosteric regulation of Hb-O_2 affinity involves the oxygenation-linked binding of nonheme ligands that indirectly modulate heme reactivity by shifting the equilibrium between a low-affinity "T-state" and a high-affinity "R-state." Allosteric cofactor molecules typically reduce Hb-O_2 affinity by preferentially binding and stabilizing deoxygenated Hb, thereby displacing the R↔T equilibrium in favor of the low-affinity T-state conformation (Fig. S2). After isolating and purifying the HbA and HbD isoforms from each hummingbird species, we measured oxygenation properties in the presence and absence of the two main allosteric effectors that regulate Hb-O_2 affinity: inositol hexaphosphate (IHP, a chemical analog of the naturally occurring inositol pentaphosphate in avian red cells, at twofold molar excess over tetrameric Hb) and Cl^- ions (added as KCl; 0.1 mol·L^{-1}). Hb-O_2 affinity was indexed by P_{50}, the PO_2 at which Hb is half-saturated. O_2-equilibrium measurements revealed that the major HbA isoforms of the high-altitude hummingbird species were generally characterized by elevated O_2-affinities in the absence of allosteric effectors ("stripped" Hb) and the difference in P_{50} values between highland and lowland species was amplified in the presence of IHP alone and in the simultaneous presence of both IHP and Cl^- ions (Table 1 and Fig. S3).

Regressions based on phylogenetically independent contrasts (PICs) revealed a significantly negative relationship between HbA P_{50} values and native elevation (i.e., a positive relationship between Hb-O_2 affinity and elevation) (Fig. 1*B* and Table S1). Similarly, for five species that expressed the HbD isoform at levels sufficient for experimental analysis, regressions based on PICs revealed significantly negative relationships between P_{50} values and native elevation, both for HbD alone and for the weighted average of HbA and HbD in their naturally occurring relative concentrations (Table S1). From this point onward, we

Table 1. Functional properties of hummingbird HbA isoforms

Species	Stripped		+KCl		+IHP		+KCl+IHP	
	P_{50}	n_{50}	P_{50}	n_{50}	P_{50}	n_{50}	P_{50}	n_{50}
Adelomyia melanogenys	2.85 ± 0.01	1.60 ± 0.00	4.60 ± 0.08	1.89 ± 0.08	28.83 ± 1.54	2.16 ± 0.14	32.02 ± 3.84	2.31 ± 0.07
Oreotrochilus estella	2.17 ± 0.12	1.36 ± 0.13	3.39 ± 0.24	1.54 ± 0.13	21.82 ± 1.09	1.98 ± 0.11	20.20 ± 0.28	2.00 ± 0.03
Oreotrochilus melanogaster	2.10 ± 0.06	1.40 ± 0.01	3.86 ± 0.05	1.75 ± 0.05	26.65 ± 0.71	2.25 ± 0.09	19.88 ± 0.27	2.08 ± 0.05
Aglaeactis castelnaudii	2.17 ± 0.06	1.38 ± 0.04	3.23 ± 0.28	1.40 ± 0.02	22.45 ± 0.93	1.51 ± 0.18	17.23 ± 0.66	1.61 ± 0.14
Coeligena coeligena	2.49 ± 0.11	1.48 ± 0.06	4.22 ± 0.16	1.67 ± 0.10	27.83 ± 0.37	1.91 ± 0.08	22.90 ± 3.16	2.19 ± 0.11
Coeligena violifer	2.12 ± 0.04	1.29 ± 0.03	3.74 ± 0.10	1.65 ± 0.08	23.55 ± 0.74	1.96 ± 0.04	19.12 ± 1.27	1.70 ± 0.19
Patagona gigas	2.52 ± 0.06	1.46 ± 0.04	4.14 ± 0.37	1.63 ± 0.13	29.97 ± 1.00	2.28 ± 0.11	25.86 ± 1.66	2.49 ± 0.42
Amazilia viridicauda	2.62 ± 0.03	1.43 ± 0.03	4.47 ± 0.05	1.81 ± 0.05	28.49 ± 1.20	2.13 ± 0.08	24.24 ± 0.87	2.07 ± 0.11
Amazilia amazilia	3.14 ± 0.43	1.38 ± 0.05	5.28 ± 0.25	1.90 ± 0.15	36.77 ± 0.85	2.16 ± 0.08	29.84 ± 0.32	2.42 ± 0.01
Phaethornis malaris	2.83 ± 0.10	1.39 ± 0.12	4.70 ± 0.06	1.83 ± 0.06	37.00 ± 0.44	2.27 ± 0.13	28.13 ± 0.60	2.04 ± 0.11

O_2-affinities (P_{50}, torr) and cooperativity coefficients (n_{50}; mean ± SEM) of purified HbA isoforms measured in 0.1 M Hepes buffer at pH 7.40 (± 0.01), 37 °C, in the absence of allosteric effectors (stripped), in the presence of KCl (0.1 M) or IHP (IHP/Hb tetramer ratio = 2.0), and in the presence of both allosteric effectors. [Heme], 0.3 mM. As explained in the text, P_{50} is an inverse measure of Hb-O_2 affinity. High-altitude species with maximum elevational ranges of >3,000 m are denoted by gray shading.

primarily focus on oxygenation properties of Hb in the presence of IHP and Cl^- ions, the experimental treatment that is most relevant to in vivo conditions in avian red cells.

Causative Substitutions and the Structural Mechanisms Underlying Evolutionary Transitions in Hb-O_2 Affinity. Inspection of the genotypic and phenotypic data suggested that phylogenetically replicated changes in Hb-O_2 affinity were largely attributable to repeated amino acid replacements at two sites: β13 (position 10 in the A helix) and β83 (position 7 in the EF interhelical segment) (Fig. 2 and Fig. S4). Within each clade, the species with the highest Hb-O_2 affinities in the presence of allosteric effectors always possessed the two-site genotype β13Ser-β83Ser (*Oreotrochilus estella*, *Oreotrochilus melanogaster*, and *P. gigas*, all of which are predominantly highland species) or β13Gly-β83Ser (*Aglaeactis castelnaudii*, *Coeligena violifer*, and *Amazilia viridicauda*, all of which are predominantly highland species), whereas the species with the lowest Hb-O_2 affinities always possessed β13Gly-β83Gly (*Adelomyia melanogenys*, *Coeligena coeligena*, *Amazilia amazilia*, and *Phaethornis malaris*, all of which are predominantly lowland species) (Fig. 2 and Table 1). Comparisons among HbD isoforms are also informative about the effects of these substitutions because HbA and HbD isoforms of the same species share identical β-chain subunits. Among the five species in which HbD was examined, the only species with the β13Ser-β83Ser genotype (the predominantly highland *P. gigas*) had the highest HbD O_2 affinity [$P_{50(KCl+IHP)}$ = 16.56 ± 0.56 torr], and the two species that shared the alternative β13Gly-β83Gly genotype (the exclusively lowland *A. amazilia* and *P. malaris*) had the two lowest affinities [$P_{50(KCl+IHP)}$ = 23.20 ± 1.21 and 24.92 ± 0.52 torr].

To identify the structural basis of variation in Hb-O_2 affinity, a comparison between the HbA isoforms of *A. melanogenys* (an exclusively lowland species) and *O. estella* (a high-altitude specialist) is especially informative because they exhibit pronounced differences in O_2-affinity [$P_{50(KCl+IHP)}$ = 32.02 ± 3.84 vs. 20.20 ± 0.28 torr, respectively] (Table 1), and yet they differ by just one conservative α-chain substitution (α8Thr→Ser) and two polarity-changing β-chain substitutions (β13Gly→Ser and β83Gly→Ser) (Fig. 2). To isolate the functional effects of the two β-chain substitutions, we used a recombinant expression vector (21) and site-directed mutagenesis to synthesize the reconstructed ancestral Coquette HbA (β13Gly-β83Gly, identical to wild-type *A. melanogenys* β-globin), the derived double-mutant genotype that is identical to wild-type *O. estella* β-globin (β13Ser-β83Ser), and each of the alternative single-mutant intermediates (β13Ser-β83Gly and β13Gly-β83Ser). Consistent with measurements of

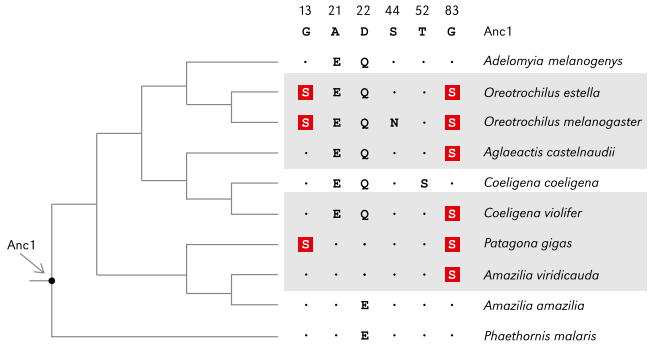

Fig. 2. Variable residue positions in a multiple alignment of hummingbird β^A-globin sequences. The estimated sequence for the common ancestor of hummingbirds (Anc1) is included for comparison, and derived Ser residues at β13 and β83 are shown in red boxes. High-altitude species with maximum elevational ranges of >3,000 m are denoted by shading. Sequences represent the most common haplotypes for each species.

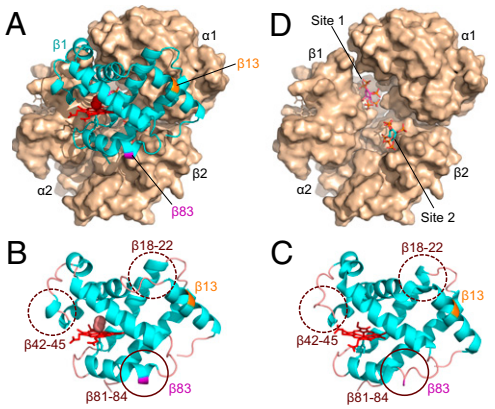

Fig. 3. Amino acid replacements at β13 and β83 produce second-order perturbations of tertiary structure that affect the allosteric regulation of O_2-binding by IHP. (*A*) Homology-based structural model of hummingbird Hb showing the locations of amino acid replacements at sites 13 and 83 in the β1 subunit (shown in cyan). β-Chain residues 18–22, 42–45, and 81–84 (including the variable site 83, the penultimate C-terminal residue in the EF interhelical loop) alternate between helical and nonhelical secondary structure in the allosteric transition between the oxy (*B*) and deoxy (*C*) states. (*D*) Structural model of hummingbird Hb (with the β1 subunit removed) showing alternative IHP-binding sites in the central cavity. Polarity-changing amino acid replacements at β13 and β83 produce nonadditive changes in the favorability of alternative conformation states for polyphosphate-binding: IHP preferentially binds at "site 1" in the β13Gly-β83Gly and β13Ser-β83Ser mutants (representing wild-type β-globin genotypes for *A. melanogenys* and *O. estella*, respectively) and at "site 2" in the β13Ser-β83Gly and β13Gly-β83Ser mutants.

the native Hbs in the presence of allosteric effectors, $P_{50(KCl+IHP)}$ for the recombinant *O. estella* Hb was significantly lower (i.e., O_2-affinity was higher) than that of *A. melanogenys* (Table S2), confirming the affinity-enhancing effect of the β13Gly→Ser and β83Gly→Ser substitutions in combination.

Epistasis for Hb-O_2 Affinity. Analysis of the alternative single- and double-mutant recombinant Hbs (rHbs) revealed that phenotypic effects of mutations at β13 and β83 are highly context-dependent; $P_{50(KCl+IHP)}$ values exhibited a significant epistatic deviation from expectations of an additive model (ε = 12.94, 95% confidence interval = 10.05–15.82). In the presence of allosteric effectors, the β13Gly→Ser substitution increased O_2-affinity on the ancestral Coquette background (in the presence of β83Gly) and reduced O_2-affinity in the presence of the derived β83Ser. Similarly, the β83Gly→Ser substitution increased O_2-affinity on the ancestral Coquette background (in the presence of β13Gly) and reduced O_2-affinity in the presence of the derived β13Ser (Table S2). This is an example of sign epistasis (22, 23), where the sign of the phenotypic effect of a mutation is conditional on the genetic background in which it occurs.

Structural Basis of Species Differences in Hb Function. To determine the structural mechanisms responsible for the additive and epistatic effects of substitutions at β13 and β83, we conducted homology-based modeling analyses of hummingbird Hb (*Methods*). These analyses revealed that Gly→Ser replacements at β13 and β83 produce localized changes in secondary structure of the A and F helices, respectively (Table S3), which impinge indirectly on the allosteric regulatory control of Hb-O_2 affinity. Site β83 is located within a segment of the β-subunit main chain (residues 81–84) that alternates between helical and nonhelical secondary structure in the allosteric transition between the oxy and deoxy states, respectively (Fig. 3 *A*–*C*). At β83, either Gly or Ser can donate a helix-capping, amide H-bond to the carbonyl oxygen of

EVOLUTION

β85Phe (the N-terminal residue of the F-helix), but the polar -OH side-chain of β83Ser forms additional intermolecular H-bonds that alter the torsion angle of the F-helix, thereby constraining allosteric movement. When nonpolar Gly is replaced by polar, hydrophilic Ser at β83 (as in the predominantly highland *Oreotrochilus*, *A. castelnaudii*, *C. violifer*, *P. gigas*, and *A. viridicauda*) (Fig. 2), the effect on Hb allostery is contingent on the presence of Gly or Ser at β13. Changes in the network of atomic contacts involving β13 and β83 (Table S3) alter the favorability of alternative conformation states for IHP-binding in the central cavity (Fig. 3*D*), and the resultant changes in the location of IHP-binding account for the observed epistasis for Hb-O_2 affinity in the presence of IHP (Table S2). Our experimental results for the hummingbird rHb mutants are consistent with functional studies of a naturally occurring human Hb mutant, Hb Pyrgos (β83Gly→Asp), which is also characterized by an increased O_2-affinity in the presence of organic phosphates (24).

Parallelism of β-Chain Substitutions Among Species. We sequenced β^A-globin in 63 hummingbird species and we then used maximum-likelihood and parsimony to map the β13 and β83 replacements onto an independently derived and well-resolved phylogeny (25). This analysis revealed that the substitutions (and, by implication, the associated changes in Hb-O_2 affinity) occurred at least 17 times independently (≥4 and ≥13 transitions between Gly and Ser at β13 and β83, respectively). Maximum-likelihood ancestral-state estimates for native elevation indicated that hummingbird species have shifted upwards and downward during the evolution of the group, in conjunction with repeated substitutions and back-substitutions at β13 and β83 (Fig. 4 and Fig. S5). Hence, the negative correlation between P_{50} and native elevation (Fig. 1*B*) is attributable to derived increases in Hb-O_2 affinity in highland lineages, as well as derived reductions in Hb-O_2 affinity in lowland lineages. For example, the common ancestor of the highland genus *Oreotrochilus* (β13Ser-β83Ser) evolved a derived increase in Hb-O_2 affinity relative to the likely ancestral state of the Coquette clade (β13Gly-β83Gly). In contrast, in the Brilliants the lowland *C. coeligena* (β13Gly-β83Gly) evolved a derived reduction in Hb-O_2 affinity relative to the likely ancestral state for that clade (β13Gly-β83Ser) (Fig. 4). Species' maximum elevation was strongly associated with β13-β83 genotype in a phylogenetic general linear model ($R^2 = 0.53$; $P < 10^{-11}$) (Fig. 4).

Among distantly related species, parallel substitutions at sites β13 and β83 are likely attributable to the repeated fixation of identical-by-state alleles that had independent mutational origins. Among some of the more closely related species, the sorting of ancestral polymorphism may produce the same pattern of parallelism because of the repeated fixation of identical-by-descent alleles in recently diverged lineages (26). Further work is needed to elucidate the mutational origins of the β13 and β83 variants, but it is clear that repeated changes at both sites have contributed to the repeated elevational shifts in Hb function among different lineages. Aside from the variation at sites β13 and β83, no other substitutions in the α^A-, α^D-, or β^A-globin genes exhibited any obvious association with species differences in P_{50} values for HbA or HbD, although it is likely that particular lineage-specific substitutions (Fig. S4) account for residual variation in Hb-O_2 affinity among species.

Possible Adaptive Significance of Altitudinal Differences in Hb-O_2 Affinity. The evolution of divergent Hb-O_2 affinities between highland and lowland hummingbirds is consistent with theoretical predictions (1–6). At low altitude, a low Hb-O_2 affinity is expected to be physiologically advantageous for hummingbirds and other animals with high mass-specific metabolic rates because O_2 unloading in the peripheral circulation can occur at relatively high PO_2, thereby optimizing tissue oxygenation by increasing the O_2 diffusion gradient between capillary blood and tissue mitochondria. At low altitude, the trade-off with pulmonary O_2 loading is alleviated because arterial O_2 saturation will still be near-maximal. However, under conditions of severe environmental hypoxia at very high altitudes, an increased Hb-O_2 affinity becomes advantageous because tissue O_2 delivery can be

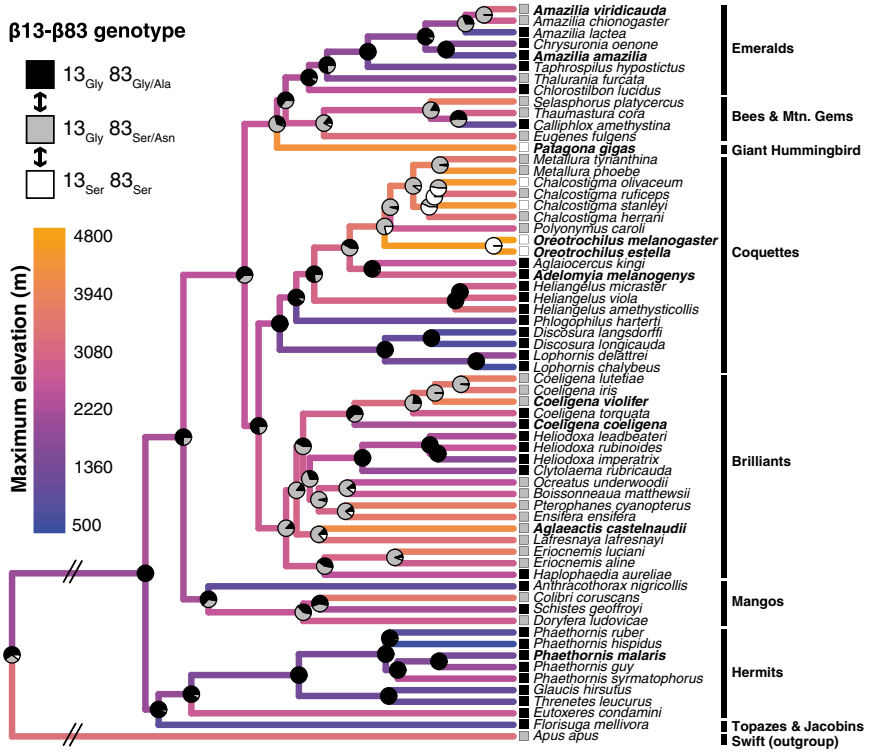

Fig. 4. Ancestral state estimates for β13 and β83 in hummingbirds. Pie diagrams at the nodes indicate the probability of each genotype based on a stepwise, single-rate maximum-likelihood model with two reversible transitions, as indicated in the inset diagram. Terminal branches of the phylogenetic tree are color-coded according to the upper limit of the species' elevational range, and internal branches are color-coded based on maximum-likelihood estimates of the ancestral states. The phylogenetically corrected association between β13-β83 genotype and native elevation was highly significant (see text for details). Parsimony analysis revealed a minimum of 17 changes in genotype across the tree (Fig. S5). β83Asn was observed in a single species, *Doryfera ludoviciae*, and was therefore binned with the β83Ser character state because side-chains of the two residues have the same polarity and the underlying codons are connected by a single mutational step. Similarly, β83Ala was observed in a single species, *Phlogophilus harterti*, and was binned with the β83Gly character state in this analysis. Branch lengths are proportional to relative time, except where indicated. Species names in bold are those that were included in the experimental analysis of Hb function.

preserved more effectively by safeguarding arterial O_2 saturation than by maximizing O_2 unloading from partially desaturated blood (1–6, 8, 9).

Mechanisms of Hb Adaptation and Causes of Parallelism at the Sequence Level. Comparative studies of Hb function in different animal species and experimental studies of naturally occurring or recombinant human Hb mutants have demonstrated that genetically based changes in Hb-O_2 affinity can be produced by numerous possible structural changes (27–29). In Andean hummingbirds, amino acid replacements at β13 and β83 contribute to species differences in Hb-O_2 affinity, but it is certainly not because they represent the only possible mutational changes that are capable of producing the observed changes in protein function. Although there may be numerous possible mutations that can produce identical changes in Hb-O_2 affinity, many of those changes are known to have deleterious pleiotropic effects. For example, active site mutations that alter the polarity or hydrophobicity of the distal heme pocket can produce direct changes in the association constant for O_2 binding, but such mutations typically compromise structural stability or increase the susceptibility to heme autoxidation (the spontaneous oxidation of the heme iron from the ferrous Fe^{2+} state to the ferric Fe^{3+} state, which renders Hb functionally inert as an O_2-transport molecule) (29). In contrast, mutations remote from the active site—like those at β13 and β83—can potentially produce fine-tuned changes in O_2-affinity with minimal pleiotropic effects through subtle displacements of the allosteric equilibrium (28–30). Within the set of all possible mutations that produce functionally equivalent effects on Hb-O_2 affinity, those that incur a lesser magnitude of deleterious pleiotropy are predicted to have a higher fixation probability, and such mutations may therefore contribute disproportionately to biochemical adaptation (31–33). When such changes are driven by positive directional selection, theory predicts that they are especially likely to evolve in parallel (34).

The parallel β13 and β83 substitutions that we have documented in hummingbirds have not been implicated in the adaptation of Hb function in other high-altitude birds or mammals (35–39), although a survey of sequence variation in the globin genes of Andean waterfowl documented a shared β13Gly/Ser polymorphism in speckled teals (*Anas flavirostris*) and yellow-billed pintails (*Anas georgica*), and in both species the derived Ser variant was present at high frequency in high-altitude populations (40). The phenotypic effects of the β13Gly/Ser variants in these waterfowl species have not yet been investigated, but the similar altitudinal patterns in Andean ducks and hummingbirds suggest parallel mechanisms of Hb evolution. At β13 and β83 in Andean hummingbirds, it may be that recurrent mutation and retention of ancestral polymorphism both contributed to variation in Hb function—variation that was then recruited when selection favored fine-tuned adjustments in blood-O_2 transport (e.g., during elevational range shifts). When closely related species independently adapt to a shared environmental challenge, natural selection may be predisposed to hit upon the same design solution in different lineages if one particularly accessible (and minimally pleiotropic) solution happens to be located within striking distance from the same ancestral starting point.

Methods

Specimen Collection. We preserved blood and tissue samples from voucher specimens of hummingbirds that were collected from numerous Andean localities spanning an elevational range of ~4,500 m (Table S4). Our analysis of Hb function was based on blood samples from 70 hummingbird specimens (n = 3–8 individuals per species). All hummingbirds were live-trapped in mistnets and were bled and killed in accordance with guidelines of the Ornithological Council (41), and protocols approved by the University of New Mexico Institutional Animal Care and Use Committee (Protocol number 08UNM033-TR-100117; Animal Welfare Assurance number A4023-01). All fieldwork was carried out under permits issued by the management authorities of Peru (76-2006-INRENA-IFFS-DCB, 087–2007-INRENA-IFFS-DCB, and 135–2009-AG-DGFFS-DGEFFS).

For each individual bird, we collected 0.03–0.20 mL of whole blood from the brachial or ulnar vein using heparinized microcapillary tubes. Red blood cells were separated from the plasma fraction by centrifugation, and the packed red cells were then snap-frozen in liquid nitrogen and were stored at −80 °C before use as a source of Hb for experimental studies. We collected liver and pectoral muscle from each specimen as sources of genomic DNA and globin mRNA, respectively. Muscle samples were snap-frozen or preserved using RNAlater and were subsequently stored at −80 °C before RNA isolation. Voucher specimens were preserved along with ancillary data and were deposited in the collections of the Museum of Southwestern Biology of the University of New Mexico and the Centro de Ornitología y Biodiversidad (CORBIDI), Lima, Peru. Complete specimen data are available via the ARCTOS online database (Table S4).

Molecular Cloning and Sequencing. We cloned and sequenced the adult globin genes (α^A-, α^D-, and β^A-globin) from at least two specimens per species. We used the RNeasy Mini Kit (Qiagen) to isolate RNA, and we used 5′ and 3′ RACE (Invitrogen Life Technologies) to obtain cDNA sequence for the 5′ and 3′ UTRs of each adult-expressed globin gene. After designing paralog-specific PCR primers with annealing sites in the 5′ and 3′ UTRs, complete cDNAs were synthesized for each gene by reverse transcription using the OneStep RT-PCR kit (Qiagen). We cloned gel-purified RT-PCR products into pCR4-TOPO vector using the TOPO TA Cloning Kit (Invitrogen Life Technologies). All new sequences were deposited in GenBank under accession nos. KF222496, KF222499, KF222501, KF222503, KF222506, and KF222510–KF222539.

Characterization of Hb Isoform Composition. We used isoelectric focusing (IEF; PhastSystem, GE Healthcare Bio-Sciences) to characterize Hb isoform composition in red cell lysates from each of the 70 hummingbird specimens. After separating native Hbs by means of IEF, gel bands were excised and digested with trypsin. The resultant peptides were then identified by means of tandem mass spectrometry (MS/MS). Database searches of the resultant MS/MS spectra were performed using Mascot (Matrix Science, v1.9.0), whereby peptide mass fingerprints were used to query a custom database of avian α- and β-chain sequences (17, 42–44), including α^A-, α^D-, and β^A-globin sequences from each of the surveyed hummingbird species. After separating the HbA and HbD isoforms by native gel IEF and identifying each of the constituent subunits by MS/MS, the relative abundance of the different isoforms in the hemolysates of each individual was quantified densitometrically using ImageJ (45).

Protein Purification and Measurement of Hb-O_2 Equilibria. The HbA and HbD isoforms (isoelectric points = 8.9–9.1 and 6.8–7.3, respectively) were separated and stripped of organic phosphates by means of ion-exchange chromatography. O_2 equilibria of purified Hb solutions [3 μL thin-layer samples, (heme) 0.3 mM] were measured at 37 °C in the presence of 0.1 M Hepes buffer (pH 7.4). To characterize the allosteric regulation of Hb-O_2 affinity, we measured O_2-equilibrium curves in the absence of allosteric effectors (stripped), in the presence of Cl^- ions (0.1 M KCl), in the presence of IHP (IHP/Hb tetramer ratio = 2.0), and in the simultaneous presence of both effectors. For details of the purification protocol and the measurement of Hb-O_2 equilibrium curves, see *SI Methods*.

Vector Construction, Site-Directed Mutagenesis, and Synthesis of rHbs. To produce rHbs for the protein engineering experiments, the α^A- and β^A-globin genes of *A. melanogenys* were synthesized by Genscript after optimizing nucleotide sequences with respect to *Escherichia coli* codon preferences. Gene cassettes for the α^A- and β^A-globin genes and the *methionine aminopeptidase* (*MAP*) gene were tandemly cloned into the custom pGM expression plasmid described by Natarajan et al. (21). All rHbs were expressed in the JM109 (DE3) *E. coli* strain. See *SI Methods* for details regarding the site-directed mutagenesis experiments, the expression and purification of the hummingbird rHb mutants, the measurement of rHb oxygenation properties, and the measurement of epistasis.

Ancestral State Estimates. To infer the polarity of character-state changes at β13 and β83, we sequenced the β^A-globin gene of 63 hummingbird species with known phylogenetic relationships. Orthologous sequence from the common swift (*Apus apus*) was used as an outgroup. Fifty-six of the 63 nodes in the independently derived phylogeny were resolved with >95% posterior probability (Dataset S1). We estimated ancestral states of the β13-β83 genotypes using maximum-likelihood and parsimony with the APE package in R (46). Two of the observed genotypes included rare variants at β83 (β13Gly-β83Asn

and β13Gly-β83Ala) that differed by a single codon change from physiochemically similar alternative states (β83Ser and β83Gly, respectively). We binned each of these singleton changes with the related codon state, resulting in three classes of two-site β13-β83 genotypes. In the maximum-likelihood model, we allowed only the two reversible transitions that each comprised a single nucleotide change. We applied a model with one rate for all transitions because likelihood ratio tests indicated that models with two to four rate parameters were not justified (46) (Fig. 4). For details regarding the phylogenetic topology and phylogenetic comparative methods, see *SI Methods*.

Structural Modeling and Molecular Docking. Homology-models of hummingbird Hb were built by the SWISS-MODEL server in the automated model (47), using *Anas platyrhynchos* Hb (PDB ID code 3EOK) as template. For each of the four rHb mutants, the root-mean-square-deviation was 0.74 Å between model and template and the QMEAN value remained between 0.70 and 0.78 for all models. Molecular docking of IHP in the Hb central cavity was performed using AutoDock Vina (48). Internal molecular contacts were identified by the Frustratometer program (49).

ACKNOWLEDGMENTS. For assistance in the field, we thank F. Angulo P., E. Bautista O., E. J. Beckman, P. M. Benham, D. Blanco, Centro de Ornitología y Biodiversidad (Lima, Peru), R. W. Dickerman, S. G. DuBay, L. M. Flores, A. B. Johnson, K. G. McCracken, J. A. Otero, A. Quiñonez Z., C. J. Schmitt, D. C. Schmitt, C. G. Schmitt, T. Valqui, W. Vargas C., B. Walker, and N. A. Wright; for assistance in the lab, we thank A. Bang (Aarhus) and A. Rutherford (Lincoln); and we thank K. G. McCracken and two anonymous reviewers for constructive comments on the manuscript. This study was supported by National Institutes of Health Grants R01 HL087216 and HL087216-S1 (to J.F.S); National Science Foundation Grants IOS-0949931 (to J.F.S.), DEB-0543556 (to J.A.M. and R.D.), and DEB-1146491 (to C.C.W.); the Danish Council for Independent Research, Natural Sciences Grant 10-084565 (to A.F.); the Center for Evolutionary and Theoretical Immunology at the University of New Mexico; and the Faculty of Science and Technology at Aarhus University.

1. Turek Z, Kreuzer F, Hoofd LJ (1973) Advantage or disadvantage of a decrease of blood oxygen affinity for tissue oxygen supply at hypoxia. A theoretical study comparing man and rat. *Pflugers Arch* 342(3):185–197.
2. Turek Z, Kreuzer F (1976) Effect of a shift of the oxygen dissociation curve on myocardial oxygenation at hypoxia. *Adv Exp Med Biol* 75:657–662.
3. Turek Z, Kreuzer F, Ringnalda BEM (1978) Blood gases at several levels of oxygenation in rats with a left-shifted blood oxygen dissociation curve. *Pflugers Arch* 376(1):7–13.
4. Turek Z, Kreuzer F, Turek-Maischeider M, Ringnalda BEM (1978) Blood O_2 content, cardiac output, and flow to organs at several levels of oxygenation in rats with a left-shifted blood oxygen dissociation curve. *Pflugers Arch* 376(3):201–207.
5. Bencowitz HZ, Wagner PD, West JB (1982) Effect of change in P_{50} on exercise tolerance at high altitude: A theoretical study. *J Appl Physiol* 53(6):1487–1495.
6. Willford DC, Hill EP, Moores WY (1982) Theoretical analysis of optimal P_{50}. *J Appl Physiol* 52(4):1043–1048.
7. Scott GR, Milsom WK (2006) Flying high: a theoretical analysis of the factors limiting exercise performance in birds at altitude. *Respir Physiol Neurobiol* 154(1-2):284–301.
8. Mairbäurl H, Weber RE (2012) Oxygen transport by hemoglobin. *Compr Physiol* 2(2): 1463–1489.
9. Storz JF, Scott GR, Cheviron ZA (2010) Phenotypic plasticity and genetic adaptation to high-altitude hypoxia in vertebrates. *J Exp Biol* 213(Pt 24):4125–4136.
10. Suarez RK, Lighton JRB, Brown GS, Mathieu-Costello O (1991) Mitochondrial respiration in hummingbird flight muscles. *Proc Natl Acad Sci USA* 88(11):4870–4873.
11. Suarez RK (1992) Hummingbird flight: Sustaining the highest mass-specific metabolic rates among vertebrates. *Experientia* 48(6):565–570.
12. Suarez RK (1998) Oxygen and the upper limits to animal design and performance. *J Exp Biol* 201(Pt 8):1065–1072.
13. Altshuler DL, Dudley R (2002) The ecological and evolutionary interface of hummingbird flight physiology. *J Exp Biol* 205(Pt 16):2325–2336.
14. McGuire JA, Witt CC, Remsen JV, Dudley R, Alshuler DL (2009) A higher-level taxonomy for hummingbirds. *J Ornithol* 150(1):155–165.
15. Weber RE, Fago A (2004) Functional adaptation and its molecular basis in vertebrate hemoglobins, neuroglobins and cytoglobins. *Respir Physiol Neurobiol* 144(2-3):141–159.
16. Storz JF, Opazo JC, Hoffmann FG (2013) Gene duplication, genome duplication, and the functional diversification of vertebrate globins. *Mol Phylogenet Evol* 66(2): 469–478.
17. Grispo MT, et al. (2012) Gene duplication and the evolution of hemoglobin isoform differentiation in birds. *J Biol Chem* 287(45):37647–37658.
18. Hiebl I, Weber RE, Schneeganss D, Kosters J, Braunitzer G (1988) Structural adaptations in the major and minor hemoglobin components of adult Ruppell's griffon (*Gyps ruepellii*, Aegypiinae): A new molecular pattern for hypoxia tolerance. *Biol Chem Hoppe Seyler* 369:217–232.
19. Weber RE, Hiebl I, Braunitzer G (1988) High altitude and hemoglobin function in the vultures *Gyps rueppellii* and *Aegypius monachus*. *Biol Chem Hoppe Seyler* 369(4): 233–240.
20. Hoffmann FG, Storz JF (2007) The αD-globin gene originated via duplication of an embryonic α-like globin gene in the ancestor of tetrapod vertebrates. *Mol Biol Evol* 24(9):1982–1990.
21. Natarajan C, et al. (2011) Expression and purification of recombinant hemoglobin in *Escherichia coli*. *PLoS ONE* 6(5):e20176.
22. Weinreich DM, Watson RA, Chao L (2005) Sign epistasis and genetic constraint on evolutionary trajectories. *Evolution* 59(6):1165–1174.
23. Natarajan C, et al. (2013) Epistasis among adaptive mutations in deer mouse hemoglobin. *Science* 340(6138):1324–1327.
24. Wajcman H, et al. (1978) Hémoglobine Pyrgos beta 83 (EF 7) Gly → Asp chez un Malien: Identification structurale et propriétés fonctionnelles. *Nouv Rev Fr Hematol* 20(3):403–411.
25. McGuire JA, Witt CC, Altshuler DL, Remsen JV, Jr. (2007) Phylogenetic systematics and biogeography of hummingbirds: Bayesian and maximum likelihood analyses of partitioned data and selection of an appropriate partitioning strategy. *Syst Biol* 56(5): 837–856.
26. Clark AG (1997) Neutral behavior of shared polymorphism. *Proc Natl Acad Sci USA* 94(15):7730–7734.
27. Weber RE (2007) High-altitude adaptations in vertebrate hemoglobins. *Respir Physiol Neurobiol* 158(2–3):132–142.
28. Storz JF, Moriyama H (2008) Mechanisms of hemoglobin adaptation to high altitude hypoxia. *High Alt Med Biol* 9(2):148–157.
29. Varnado CL, et al. (2013) Development of recombinant hemoglobin-based oxygen carriers. *Antioxid Redox Signal* 18(17):2314–2328.
30. Maillett DH, et al. (2008) Interfacial and distal-heme pocket mutations exhibit additive effects on the structure and function of hemoglobin. *Biochemistry* 47(40): 10551–10563.
31. Otto SP (2004) Two steps forward, one step back: The pleiotropic effects of favoured alleles. *Proc Biol Sci* 271(1540):705–714.
32. Stern DL, Orgogozo V (2009) Is genetic evolution predictable? *Science* 323(5915): 746–751.
33. Streisfeld MA, Rausher MD (2011) Population genetics, pleiotropy, and the preferential fixation of mutations during adaptive evolution. *Evolution* 65(3):629–642.
34. Orr HA (2005) The probability of parallel evolution. *Evolution* 59(1):216–220.
35. Jessen T-H, Weber RE, Fermi G, Tame J, Braunitzer G (1991) Adaptation of bird hemoglobins to high altitudes: Demonstration of molecular mechanism by protein engineering. *Proc Natl Acad Sci USA* 88(15):6519–6522.
36. Weber RE, Jessen T-H, Malte H, Tame J (1993) Mutant hemoglobins (α^{119}-Ala and β^{55}-Ser): functions related to high-altitude respiration in geese. *J Appl Physiol (1985)* 75(6):2646–2655.
37. Storz JF, et al. (2009) Evolutionary and functional insights into the mechanism underlying high-altitude adaptation of deer mouse hemoglobin. *Proc Natl Acad Sci USA* 106(34):14450–14455.
38. Storz JF, Runck AM, Moriyama H, Weber RE, Fago A (2010) Genetic differences in hemoglobin function between highland and lowland deer mice. *J Exp Biol* 213(Pt 15): 2565–2574.
39. Revsbech IG, et al. (2013) Hemoglobin function and allosteric regulation in semifossorial rodents (family Sciuridae) with different altitudinal ranges. *J Exp Biol* 216(Pt 22): 4264–4271.
40. McCracken KG, et al. (2009) Parallel evolution in the major haemoglobin genes of eight species of Andean waterfowl. *Mol Ecol* 18(19):3992–4005.
41. Fair JM, Paul E (2010) *Guidelines to the Use of Wild Birds in Research*, ed Jones J (Ornithological Council, Washington, DC).
42. Hoffmann FG, Storz JF, Gorr TA, Opazo JC (2010) Lineage-specific patterns of functional diversification in the α- and β-globin gene families of tetrapod vertebrates. *Mol Biol Evol* 27(5):1126–1138.
43. Hoffmann FG, Opazo JC, Storz JF (2011) Differential loss and retention of cytoglobin, myoglobin, and globin-E during the radiation of vertebrates. *Genome Biol Evol* 3: 588–600.
44. Hoffmann FG, Opazo JC, Storz JF (2012) Whole-genome duplications spurred the functional diversification of the globin gene superfamily in vertebrates. *Mol Biol Evol* 29(1):303–312.
45. Abramoff MD, Magelhaes PJ, Ram SJ (2004) Image processing with Image J. *Biophotonics International* 11(7):36–42.
46. Paradis E, Claude J, Strimmer K (2004) APE: Analyses of phylogenetics and evolution in R language. *Bioinformatics* 20(2):289–290.
47. Arnold K, Bordoli L, Kopp J, Schwede T (2006) The SWISS-MODEL workspace: A web-based environment for protein structure homology modelling. *Bioinformatics* 22(2): 195–201.
48. Trott O, Olson AJ (2010) AutoDock Vina: Improving the speed and accuracy of docking with a new scoring function, efficient optimization, and multithreading. *J Comput Chem* 31(2):455–461.
49. Jenik M, et al. (2012) Protein frustratometer: A tool to localize energetic frustration in protein molecules. *Nucleic Acids Res* 40(Web Server issue):W348–W351.

Supporting Information

Projecto-Garcia et al. 10.1073/pnas.1315456110

SI Methods

Protein Purification. The HbA and HbD isoforms were separated by passing the samples through an ion-exchange chromatography column (HiTrap QHP, 5 × 1 mL, 17–1153-01; GE Healthcare) equilibrated with 20 mM Tris buffer (pH 8.2) and eluted using a linear gradient of 0–0.2 M NaCl. Samples were desalted by overnight dialysis against three changes of 10 mM Hepes buffer (pH 7.6) at 4 °C. Samples were concentrated (to >1 mM heme) using Millipore centrifugal filter units (MW = 30,000; Millipore) at 7,000 × *g* before freezing at −80 °C. Heme oxy concentration (millimolar) was calculated from the absorbance peaks in the visible region of the spectrum (577 nm and 540 nm) using standard extinction coefficients.

Hb-O_2 Equilibria. O_2-equilibrium curves were measured using a modified O_2 diffusion chamber where changes in absorption (436 nm) of ultrathin (~1.4 μm) layers of Hb solutions were recorded following complete oxygenation (100% saturation) and deoxygentation (0% saturation) of Hb, achieved via equilibration with pure O_2 and N_2, respectively, and complete equilibration to gas mixtures of varying O_2 tension generated by precision Wösthoff gas-mixing pumps, as described previously (1–3). Values of P_{50} and n_{50} (Hill's cooperativity coefficient at half-saturation) were interpolated from the linear portion of Hill plots [log ([HbO_2]/[Hb] vs. log PO_2] based on four to six equilibration steps between 30% and 70% oxygenation. Free Cl^- concentrations were measured with a model 926S Mark II chloride analyzer (Sherwood Scientific). We used standard concentrations of Cl^- (0.1 M KCl) and inositol hexaphosphate (IHP; IHP/Hb tetramer ratio = 2.0) (4, 5) that closely approximate intraerythrocytic effector concentrations in vivo (6–8). Predicted P_{50}s of composite hemolysates were calculated as the average value for HbA and HbD, weighted according to the naturally occurring relative concentration of each isoform.

Vector Construction and Site-Directed Mutagenesis. The α^A- and β^A-globin genes of *Adelomyia melanogenys* were synthesized by Genscript after optimizing nucleotide sequences with respect to *Escherichia coli* codon preferences. Gene cassettes for the α^A- and β^A-globin genes and the *methionine aminopeptidase* (*MAP*) gene were tandemly cloned into the custom pGM expression plasmid described by Natarajan et al. (9). To maximize efficiency in the posttranslational cleaving of N-terminal methionines from the α- and β-chain polypeptides, an additional copy of the *MAP* gene was cloned into the pCO-MAP plasmid with a kanamycin resistant gene and was coexpressed with the pGM expression plasmid.

The *A. melanogenys* β^A-globin was converted into the *Oreotrochilus estella* sequence by engineering two codon changes (β13Gly→Ser and β83Gly→Ser) using site-directed mutagenesis. The same procedure was used to engineer the two possible mutational intermediates between the β-chain Hbs of the two species (β13Ser-β83Gly and β13Gly-β83Ser). The mutagenesis experiments were performed with the QuikChange II XL Site-Directed Mutagenesis kit from Stratagene in accordance with the manufacturer's protocol. The presence of each engineered codon change was verified by DNA sequencing. In addition to the two above-mentioned β-chain substitutions, the major Hb isoforms of *A. melanogenys* and *O. estella* are also distinguished from one another by a single conservative α-chain substitution. We retained the *A. melanogenys* character state at this site (α8Thr) in all engineered rHbs to control for the effects of substitutions at β13 and β83.

Expression, Purification, and Functional Analysis of Recombinant Hemoglobins. All recombinant hemoglobins (rHbs) were expressed in the JM109 (DE3) *E. coli* strain and the bacterial cells were subject to dual selection in an LB agar plate containing ampicillin and kanamycin to ensure that the transformants receive both the pGM and pCO-MAP plasmids. Large-scale production was conducted in 1- to 1.5-L batches containing TB medium. Cells were grown at 37 °C in an orbital shaker at 200 rpm until absorbance values reached 0.6–0.8 at 600 nm. The cells were induced with 0.2 mM isfopropyl-β-D-thiogalactopyranoside (IPTG) and were then supplemented with hemin (50 μg/mL) and glucose (20 g/L). The cells were then subsequently grown at 28° C for 16 h in an orbital shaker at 200 rpm. The bacterial culture was saturated with CO for 15 min and the cells were harvested by centrifugation and stored at −80 °C. Subsequently the cells were resuspended in lysis buffer (3 mL/g of cells, 50 mM Tris base, 1 mM EDTA, 0.5 mM DTT) and lysozyme (1 mg/g cells) was added before sonication. Polyethyleneimine solution (0.5–1%) was added to the crude lysates to precipitate nucleic acids. After centrifugation (15,000 × *g* for 45 min at 4 °C), the clarified supernatants were dialyzed overnight against three changes of 20 mM Tris buffer (0.5 mM EDTA, 0.5 mM DTT, pH 7.6) at 4 °C. Centrifugation at 14,000 × *g* was used to pellet cell debris. Recombinant Hbs were then purified in a two-step process using ion-exchange chromatography. In the first step, the sample was passed through a column (HiTrap SPHP, 5 × 5 mL, 17–1152-01) equilibrated with 20 mM Tris buffer (0.5 mM EDTA, 0.5 mM DTT, pH 6.0) and was eluted using a linear gradient of 0–0.5 M NaCl. In the second step the sample was passed through another ion-exchange column (HiTrap QHP, 5 × 5 mL, 17–1153-01; GE Healthcare) equilibrated with 20 mM Tris buffer (0.5 mM EDTA, 0.5 mM DTT, pH 8.5) and was eluted using a linear gradient of 0–0.5 M NaCl. Samples were desalted by overnight dialysis against three changes of 10 mM Hepes buffer (pH 7.6) at 4 °C. If necessary, samples were concentrated to >1 mM heme using Millipore centrifugal filter units (MW = 30,000; Millipore) at 7000 × *g* before freezing at −80 °C. As a means of quality assessment, absorbance spectra of oxy, deoxy, and CO derivatives were measured at 450–600 nm to confirm that the absorbance maxima of rHb mutants corresponded to those of the native Hbs. O_2-binding equilibria of rHb solutions were measured using the same protocol described above for the native Hb samples, and we used an enzymatic metHb reductase system (10) to maintain heme iron in the ferrous Fe^{2+} state. The measured P_{50} values for the native Hbs were based on pooled samples from multiple individuals per species, so allelic variation in the α- and β-chain subunits contributes to discrepancies in measured P_{50} values between the native Hbs, which have a heterogeneous amino acid composition, and the recombinant Hbs, which have an invariant amino acid composition.

Measurement of Epistasis. For the set of four rHb mutants representing each possible two-site combination of amino acid substitutions at β13 and β83, we tested for epistatic deviations from the expectations of an additive model: $\varepsilon = (P_{ii} + P_{jj}) - (P_{ij} + P_{ji})$, where P_{ij} is the measured P_{50} of the rHb with substitutions *i* and *j* at each site. The SE of the measured epistatic deviation, a linear function of P_{ij}, was calculated using the method of error propagation:

$\sigma_\varepsilon = \sqrt{\sigma P_{ii}^2 + \sigma P_{jj}^2 + \sigma P_{ij}^2 + \sigma P_{ji}^2}$, and the 95% confidence interval for ε was computed as $\varepsilon \pm \sigma_\varepsilon \times 1.96$ (11). Epistasis between a given pair of sites was considered to be statistically significant if the 95% confidence interval for ε did not include zero.

Phylogenetically Independent Contrasts. We used a four-gene DNA sequence alignment for 151 species of hummingbirds (12), augmented with 143 additional species and two additional nuclear genes to estimate an ultrametric phylogeny using BEAST (13), with branch-lengths scaled to relative time (Dataset S1). For the 10 species that were used in the experimental studies of Hb function, we calculated phylogenetically independent contrasts (PICs) of P_{50} values and regressed them against PICs of native elevation. All nodes in the phylogeny of these 10 focal species were resolved with 100% posterior probability. Elevational range data were primarily taken from Parker et al. (14). Results were consistent whether we used the maximum, midpoint, or minimum of the species' elevational range or the actual elevation at which the specimens were collected.

1. Weber RE (1981) Cationic control of oxygen affinity in lugworm erythocruorin. *Nature* 292(5821):386–387.
2. Weber RE (1992) Use of ionic and zwitterionic (Tris/BisTris and HEPES) buffers in studies on hemoglobin function. *J Appl Physiol (1985)* 72(4):1611–1615.
3. Weber RE, et al. (2004) Modulation of red cell glycolysis: Interactions between vertebrate hemoglobins and cytoplasmic domains of band 3 red cell membrane proteins. *Am J Physiol Regul Integr Comp Physiol* 287(2):R454–R464.
4. Imai K (1982) *Allosteric Effects in Haemoglobin* (Cambridge Univ Press, Cambridge, UK).
5. Mairbäurl H, Weber RE (2012) Oxygen transport by hemoglobin. *Compr Physiol* 2(2): 1463–1489.
6. Isaacks RE, et al. (1976) Studies on avian erythrocyte metabolism-IV. relationship between the major phosphorylated metabolic intermediates and oxygen affinity of whole blood in adults and embryos in several galliformes. *Comp Biochem Physiol A* 55(1):29–33.
7. Petschow D, et al. (1977) Causes of high blood O_2 affinity of animals living at high altitude. *J Appl Physiol* 42(2):139–143.
8. Maginniss LA (1985) Red cell organic phosphates and Bohr effects in house sparrow blood. *Respir Physiol* 59(1):93–103.
9. Natarajan C, et al. (2011) Expression and purification of recombinant hemoglobin in *Escherichia coli*. *PLoS ONE* 6(5):e20176.
10. Hayashi A, Suzuki T, Shin M (1973) An enzymic reduction system for metmyoglobin and methemoglobin, and its application to functional studies of oxygen carriers. *Biochim Biophys Acta* 310(2):309–316.
11. Natarajan C, et al. (2013) Epistasis among adaptive mutations in deer mouse hemoglobin. *Science* 340(6138):1324–1327.
12. McGuire JA, Witt CC, Altshuler DL, Remsen JV, Jr. (2007) Phylogenetic systematics and biogeography of hummingbirds: Bayesian and maximum likelihood analyses of partitioned data and selection of an appropriate partitioning strategy. *Syst Biol* 56(5): 837–856.
13. Drummond AJ, Rambaut A (2007) BEAST: Bayesian evolutionary analysis by sampling trees. *BMC Evol Biol* 7:214.
14. Parker TA, Stotz DF, Fitzpatrick JW (1996) in *Neotropical Bird Ecology and Conservation*, eds Parker TA, Moskovits DK (Univ Chicago Press, Chicago), pp. 113–436.

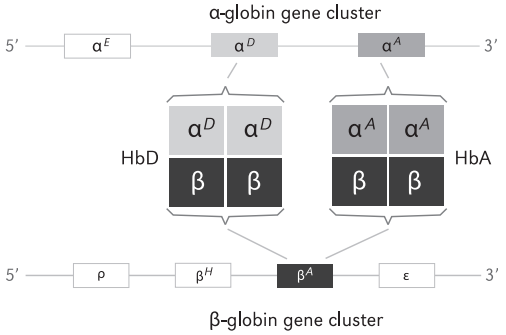

Fig. S1. Postnatally expressed Hb isoforms in avian red blood cells. The major isoform, HbA $(\alpha^A{}_2\beta_2)$, has α-type subunits encoded by the α^A-globin gene, and the minor isoform, HbD $(\alpha^D{}_2\beta_2)$, has α-type subunits encoded by the α^D-globin gene. Both isoforms share identical β-type subunits encoded by the β^A-globin gene. The remaining members of the α- and β-globin gene families (α^E-, ρ-, β^H, and ε-globin) are not expressed at appreciable levels in the definitive erythrocytes of adult birds. Within each gene cluster, the intergenic spacing is not drawn to scale.

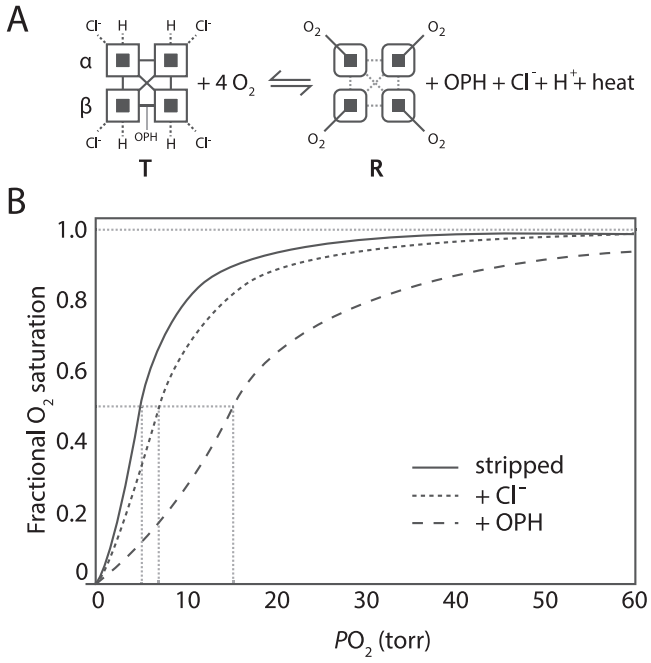

Fig. S2. Diagram illustrating the allosteric regulation of Hb-O_2 affinity. (*A*) The oxygenation reaction of tetrameric Hb ($\alpha_2\beta_2$) involves an allosteric transition in quaternary structure from the low-affinity T-state to the high-affinity R-state. The oxygenation-induced T→R transition entails a breakage of salt bridges and hydrogen bonds within and between subunits (open squares), dissociation of allosterically bound organic phosphates (OPHs), Cl^- ions, and protons, and the release of heat (heme oxygenation is an exothermic reaction). Deoxygenation-linked proton binding occurs at multiple residues in the α- and β-chains, Cl^- binding mainly occurs at the N-terminal α-amino groups of the α- and β-chains in addition to other residues in both chains, and phosphate binding occurs between the β-chains in the central cavity of the Hb tetramer. (*B*) O_2-equilibrium curves for purified Hb in the absence of allosteric effectors (stripped) and in the presence of chloride ions (+Cl^-) and organic phosphates (+OPH). The preferential binding of allosteric effectors to deoxyHb stabilizes the T-state, thereby shifting the allosteric equilibrium in favor of the low-affinity quaternary structure. The O_2-equilibrium curves are therefore right-shifted (Hb-O_2 affinity is reduced) in the presence of allosteric effectors. Hb-O_2 affinity is indexed by the P_{50} value, the PO_2 at which Hb is half-saturated. The sigmoidal shape of the O_2-equilibrium curves reflects cooperative O_2-binding, involving a PO_2-dependent shift from low- to high-affinity conformations.

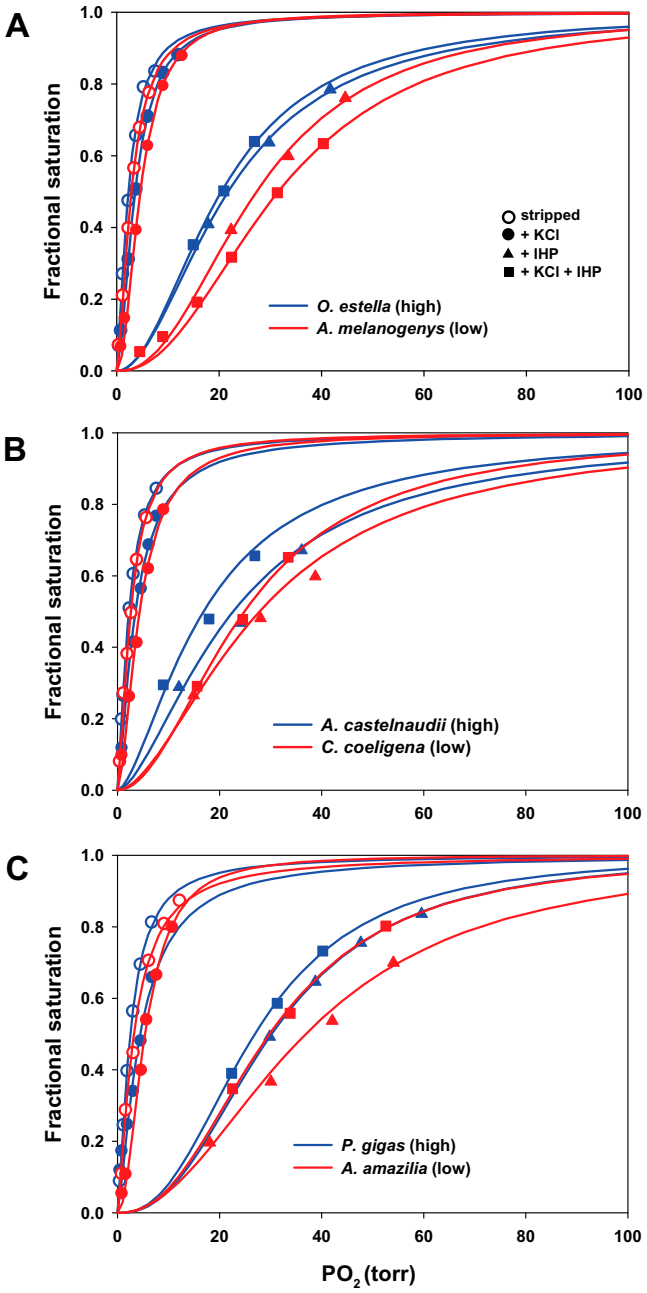

Fig. S3. O_2-equilibrium curves for purified HbA isoforms of high- and low-altitude hummingbird species. (*A*) Within the Coquettes, the Andean hillstar (*Oreotrochilus estella*), a montane species that occurs at elevations up to ~4,600 m, has a much higher Hb-O_2 affinity (i.e., a left-shifted O_2-equilibrium curve) relative to the speckled hummingbird (*Adelomyia melanogenys*), which is a middle-elevation species (1,000–2,900 m). (*B*) Within the Brilliants, the white-tufted sunbeam (*Aglaeactis castelnaudii*), a montane species that occurs at elevations up to ~4,600 m, has a much higher Hb-O_2 affinity relative to the bronzy Inca (*Coeligena coeligena*), which is native to the subtropical zone (1,000–2,200 m). (*C*) The giant hummingbird (*Patagona gigas*), which occurs at elevations up to ~4,300 m, has a higher Hb-O_2 affinity than the Amazilia hummingbird (*A. amazilia*), which is generally restricted to sea-level environments. See Table 1 for a summary of data on Hb function for all 10 species.

	α^A-globin										α^D-globin																β^A-globin					
	8	13	15	22	23	28	69	70	76	83	11	13	15	16	26	30	34	38	55	90	101	111	115	116	118	121	139	13	21	22	44	52	83
Common swift, *Apus apus*	T	V	A	E	A	A	A	A	I	L	Q	V	D	K	A	Q	T	Q	I	N	L	T	K	D	T	I	K	G	A	D	S	T	S
Adelomyia melanogenys	·	·	·	·	·	T	·	V	·	·	T	·	·	·	·	T	V	T	V	·	·	·	·	·	·	V	E	·	E	Q	·	·	G
Oreotrochilus estella	S	·	·	·	·	T	·	V	·	·	T	·	·	·	·	T	V	T	·	·	·	·	·	·	·	·	·	S	E	Q	·	·	·
Oreotrochilus melanogaster	S	·	·	·	·	T	·	V	·	·	T	·	·	·	·	T	V	T	·	·	·	·	·	·	·	·	·	S	E	Q	N	·	·
Aglaeactis castelnaudii	·	L	G	D	·	T	·	V	·	·	S	I	·	·	·	T	V	·	·	·	·	·	·	·	S	V	·	·	E	Q	·	·	·
Coeligena coeligena	·	L	G	·	·	·	·	·	·	·	S	·	·	·	V	T	V	·	·	D	P	·	E	G	S	V	·	·	E	Q	·	S	G
Coeligena violifer	·	L	G	·	·	·	·	V	M	·	S	I	·	R	·	T	V	·	·	·	·	·	·	·	S	V	·	·	E	Q	·	·	·
Patagona gigas	·	·	·	·	·	T	·	V	·	·	S	·	·	·	·	T	V	T	·	·	·	·	·	·	·	V	E	S	·	·	·	·	·
Amazilia viridicauda	·	I	·	·	D	T	·	V	·	·	T	I	E	·	·	T	V	·	V	·	·	·	·	·	·	V	·	·	·	·	·	·	·
Amazilia amazilia	·	I	·	·	D	T	·	V	·	·	T	I	E	·	·	A	V	·	V	·	·	·	·	·	·	V	·	·	·	E	·	·	G
Phaethornis malaris	·	I	·	·	D	T	P	V	·	F	A	I	·	·	·	T	A	·	V	·	·	S	·	E	·	V	·	·	·	E	·	·	G

Fig. S4. Variable residue positions in a multiple alignment of hummingbird globin sequences. Orthologous sequences from the common swift (*Apus apus*) are included for comparison. High-altitude species with maximum elevational ranges of >3,000 m are denoted by shading. Sequences represent the most common haplotypes for each species. Across all three adult-expressed globin genes (α^A-, α^D-, and β-globin), 33 of 428 amino acid sites are variable. Of the 33 variable sites, 12 have undergone repeated changes (parallelisms or reversals). Of those 12 sites, only β13 and β83 have undergone repeated amino acid replacements that are significantly associated with shifts in elevation (see text for details).

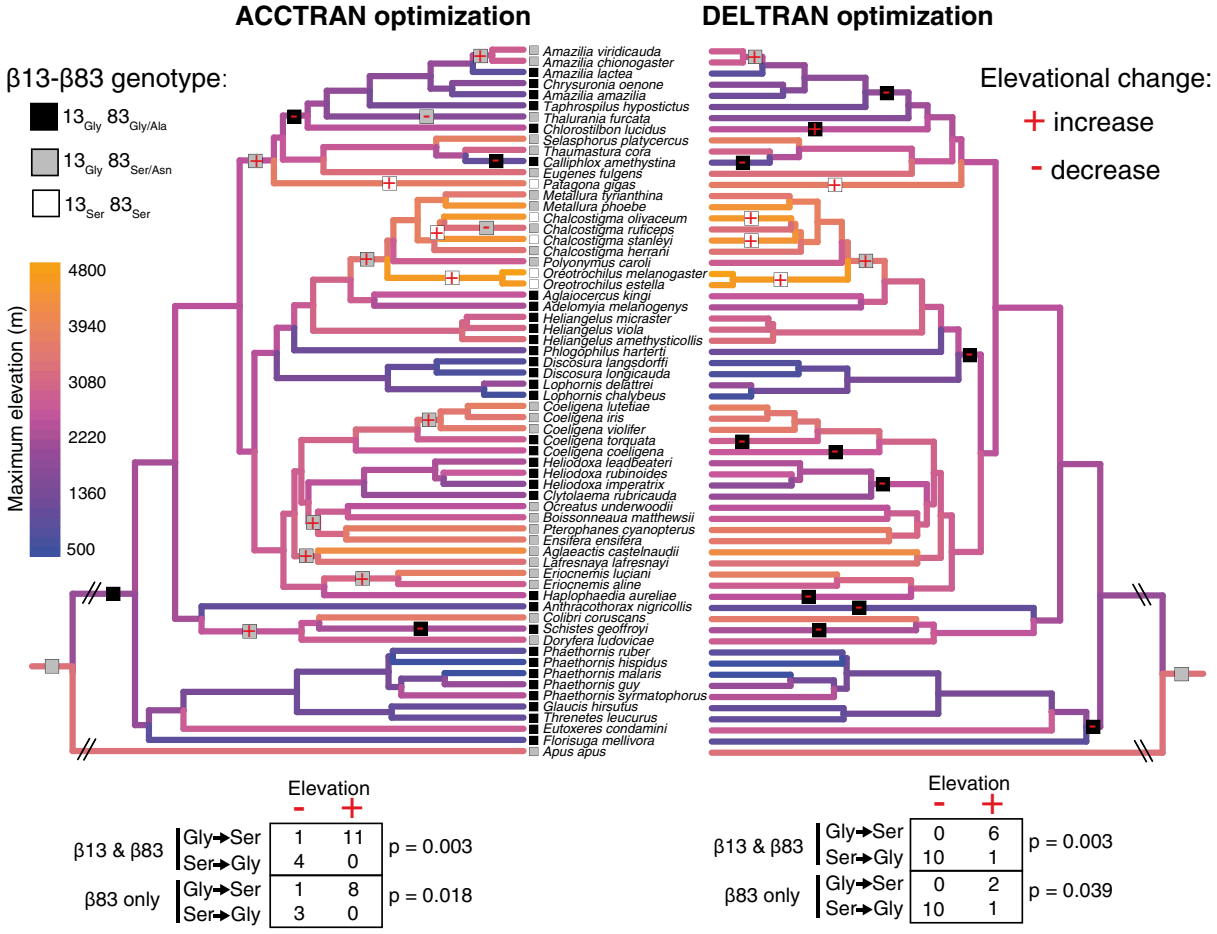

Fig. S5. Parsimony reconstructions reveal repeated substitutions and back-substitutions at β13 and β83 that are coincident with elevational range shifts during the diversification of Andean hummingbirds. Parsimony reconstructions of β13-β83 genotype were performed using accelerated (ACCTRAN) and delayed (DELTRAN) optimization to maximize reversals and parallel changes, respectively. The minimum number of transitions between Gly and Ser across the phylogeny of these 63 hummingbird species is 17, including 13 changes at β83 and 4 changes at β13. Regardless of the optimization scheme, Gly→Ser replacements at both sites are associated with upward shifts in elevation (+ symbols) relative to the immediate ancestor, whereas Ser→Gly replacements are associated with downward shifts in elevation (– symbols). In the ACCTRAN optimized scenario, the change that maps to the common ancestor of all hummingbirds is not associated with any inferred elevation change, which is why only 16 changes were included in the contingency table. Ancestral states for maximum elevation were estimated using maximum-likelihood.

Table S1. Linear regressions of Hb-O_2 affinity (P_{50}, torr) vs. native elevation for South American hummingbirds

		PIC		Nonphylogenetic	
X	Y	R^2	*P value*	R^2	*P value*
Midpoint elevation	HbA (stripped)	0.884	5.3×10^{-5}	0.842	1.8×10^{-4}
	HbA (+KCl)	0.538	0.016	0.796	0.001
	HbA (+IHP)	0.430	0.040	0.802	0.001
	HbA (+KCl+IHP)	0.737	0.001	0.651	0.005
	HbD (stripped)	0.877	0.019	0.820	0.034
	HbD (+KCl)	0.767	0.052	0.955	0.004
	HbD (+IHP)	0.890	0.016	0.851	0.026
	HbD (+KCl+IHP)	0.779	0.047	0.800	0.041
	HbA+HbD (stripped)	0.973	0.002	0.970	0.006
	HbA+HbD (+KCl)	0.928	0.008	0.887	0.017
	HbA+HbD (+IHP)	0.995	1.5×10^{-4}	0.995	1.4×10^{-4}
	HbA+HbD (+KCl+IHP)	0.983	9.7×10^{-4}	0.969	0.002
Maximum elevation	HbA (stripped)	0.800	4.7×10^{-4}	0.749	0.001
	HbA (+KCl)	0.497	0.023	0.754	0.001
	HbA (+IHP)	0.384	0.056	0.710	0.002
	HbA (+KCl+IHP)	0.581	0.010	0.512	0.020
	HbD (stripped)	0.978	0.001	0.949	0.005
	HbD (+KCl)	0.967	0.003	0.956	0.004
	HbD (+IHP)	0.987	0.001	0.974	0.002
	HbD (+KCl+IHP)	0.889	0.016	0.926	0.009
	HbA+HbD (stripped)	0.865	0.022	0.793	0.043
	HbA+HbD (+KCl)	0.947	0.005	0.904	0.013
	HbA+HbD (+IHP)	0.893	0.015	0.855	0.024
	HbA+HbD (+KCl+IHP)	0.787	0.045	0.714	0.072

Analysis of the HbA isoform was based on data from all 10 species, whereas the analysis of HbD and the weighted average of both isoforms (HbA+HbD) was based on data from a subset of five species (see main text for details). Coefficients of determination (R^2) and associated *P* values are given for regressions based on phylogenetically independent contrasts (PICs) and ordinary least-squares regressions that treat values for each species as independent datapoints. Results are shown for PIC and nonphylogenetic regressions using the midpoints and upper limits of the species-typical elevational ranges.

Table S2. Functional properties of recombinant hummingbird HbA mutants

	Stripped		+ IHP		+ KCl + IHP	
rHb mutant	P_{50}	n_{50}	P_{50}	n_{50}	P_{50}	n_{50}
β13Gly-β83Gly	2.74 ± 0.03	1.33 ± 0.04	24.22 ± 0.90	2.03 ± 0.17	19.38 ± 0.41	1.42 ± 0.07
β13Ser-β83Gly	3.21 ± 0.14	1.40 ± 0.03	13.79 ± 0.24	1.52 ± 0.10	10.99 ± 0.06	1.50 ± 0.11
β13Gly-β83Ser	3.08 ± 0.06	1.42 ± 0.02	16.73 ± 0.65	1.52 ± 0.10	11.76 ± 1.09	1.36 ± 0.06
β13Ser-β83Ser	3.21 ± 0.06	1.55 ± 0.07	24.70 ± 0.40	1.98 ± 0.08	16.31 ± 0.90	1.89 ± 0.11

O_2-affinities (P_{50}, torr) and cooperativity coefficients (n_{50}; mean ± SEM) measured in 0.1 M Hepes buffer at pH 7.40, 37 °C. Measurements were conducted in the absence of allosteric effectors (stripped), in the presence of IHP (IHP/Hb tetramer ratio = 2.0), and in the presence of both KCl (0.1 M) and IHP. [Heme], 0.3 mM.

Table S3. Variation among hummingbird β-globin variants in the nature of atomic contacts involving residue positions β13 and β83

Hb	Res 1	Res 2	CF	MF	SASA1	SASA2	Interaction
β13Gly-β83Gly	13G	15W	−0.215	−0.208	0.493	0.252	Short
	13G	16G	−0.818	−0.673	0.493	0.827	Short
	13G	17K	−0.910	−0.636	0.493	0.618	Water
	13G	18V	−1.324	0.792	0.493	0.107	Water
	13G	75V	−0.245	0.796	0.493	0.099	Water
	13G	126C	−0.875	0.763	0.493	0.048	Long
	83G	85F	−0.385	−0.315	0.613	0.028	Short
	83G	86A	−1.569	−1.227	0.613	0.432	Short
	83G	87Q	−1.113	−0.898	0.613	0.844	Water
	83G	89S	0.070	−0.766	0.613	0.020	Long
	83G	140A	−0.248	0.316	0.613	0.029	Long
	83G	143R	0.511	−0.895	0.613	0.440	Water
β13Ser-β83Ser	13S	15W	−0.172	−0.572	0.535	0.252	Water
	13S	16G	−1.223	−1.082	0.535	0.824	Water
	13S	17K	−0.874	−0.957	0.535	0.588	Water
	13S	121D	−1.203	−0.141	0.535	0.602	Water
	13S	126C	−0.560	0.680	0.535	0.048	Long
	83S	85F	−0.185	−0.399	0.631	0.028	Long
	83S	86A	−1.672	−1.011	0.631	0.427	Short
	83S	140A	−0.312	0.365	0.631	0.029	Long
β13Ser-β83Gly	13S	15W	−0.220	−0.573	0.535	0.252	Water
	13S	16G	−1.184	−1.102	0.535	0.824	Water
	13S	17K	−0.796	−0.949	0.535	0.588	Water
	13S	121D	−1.211	−0.141	0.535	0.602	Water
	13S	126C	−0.561	0.640	0.535	0.048	Long
	83G	85F	−0.429	−0.303	0.609	0.028	Short
	83G	86A	−1.571	−1.143	0.609	0.432	Short
	83G	87Q	−1.128	−0.934	0.609	0.844	Water
	83G	89S	−0.000	−0.811	0.609	0.020	Long
	83G	140A	−0.267	0.338	0.609	0.029	Long
	83G	143R	0.395	−0.854	0.609	0.440	Water
β13Gly-β83Ser	13G	15W	−0.199	−0.198	0.493	0.252	Short
	13G	16G	−0.847	−0.703	0.493	0.827	Short
	13G	17K	−0.863	−0.700	0.493	0.618	Water
	13G	18V	−1.247	0.736	0.493	0.107	Water
	13G	75V	−0.221	0.754	0.493	0.099	Water
	13G	126C	−0.821	0.844	0.493	0.048	Long
	83S	85F	−0.179	−0.404	0.631	0.028	Long
	83S	86A	−1.798	−1.148	0.631	0.429	Short
	83S	140A	−0.264	0.321	0.631	0.029	Long

β13Gly-β83Gly and β13Ser-β83Ser represent the wild-type genotypes of *A. melanogenys* and *O. estella*, respectively, and the other two genotypes represent mutational intermediates. Res 1 and 2 are identities of residues forming the contact (numbered from 1 to N). CF, configurational frustration index, which measures the interaction free energy for a given pair of native residues relative to the interaction free energies of all possible amino acid site-pairs in a similarly compact structure; MF, mutational frustration index, which measures the interaction free energy for a given pair of native residues relative to the interaction free energies between all possible amino acid site-pairs with the same coordinates; SASA1 and 2, solvent accessible surface area fractions for sites 1 and 2, respectively. Interaction: type of atomic contact: short range (short), long range (long), mediated by water molecule (water).

Table S4. Voucher specimens of South American hummingbirds used in the experimental analysis of Hb function

Species	Elevation (m)	NK tissue no.	MSB catalog number and direct Weblink to specimen data
Adelomyia melanogenys	1,395	161266	http://arctos.database.museum/guid/MSB:Bird:27492
Adelomyia melanogenys	1,395	161331	http://arctos.database.museum/guid/MSB:Bird:27552
Adelomyia melanogenys	2,102	163564	http://arctos.database.museum/guid/MSB:Bird:31892
Adelomyia melanogenys	2,111	163645	http://arctos.database.museum/guid/MSB:Bird:31973
Adelomyia melanogenys	2,052	163657	http://arctos.database.museum/guid/MSB:Bird:31985
Adelomyia melanogenys	2,144	163756	http://arctos.database.museum/guid/MSB:Bird:32084
Adelomyia melanogenys	2,147	163838	http://arctos.database.museum/guid/MSB:Bird:32166
Aglaeactis castelnaudii	4,470	159782	http://arctos.database.museum/guid/MSB:Bird:27124
Aglaeactis castelnaudii	4,330	159783	http://arctos.database.museum/guid/MSB:Bird:27125
Aglaeactis castelnaudii	4,030	159798	http://arctos.database.museum/guid/MSB:Bird:27140
Aglaeactis castelnaudii	4,330	159801	http://arctos.database.museum/guid/MSB:Bird:27143
Aglaeactis castelnaudii	4,470	159808	http://arctos.database.museum/guid/MSB:Bird:27149
Aglaeactis castelnaudii	4,300	159809	http://arctos.database.museum/guid/MSB:Bird:27150
Aglaeactis castelnaudii	4,578	169373	http://arctos.database.museum/guid/MSB:Bird:34147
Amazilia amazilia	366	162007	http://arctos.database.museum/guid/MSB:Bird:27595
Amazilia amazilia	366	162009	http://arctos.database.museum/guid/MSB:Bird:27597
Amazilia amazilia	366	162020	http://arctos.database.museum/guid/MSB:Bird:27604
Amazilia amazilia	366	162024	http://arctos.database.museum/guid/MSB:Bird:27608
Amazilia amazilia	366	162026	http://arctos.database.museum/guid/MSB:Bird:31222
Amazilia amazilia	366	162027	http://arctos.database.museum/guid/MSB:Bird:31223
Amazilia amazilia	352	163017	http://arctos.database.museum/guid/MSB:Bird:31453
Amazilia amazilia	132	168989	http://arctos.database.museum/guid/MSB:Bird:33763
Amazilia amazilia	115	169303	http://arctos.database.museum/guid/MSB:Bird:34077
Amazilia viridicauda	3,005	159899	http://arctos.database.museum/guid/MSB:Bird:27227
Amazilia viridicauda	3,005	159900	http://arctos.database.museum/guid/MSB:Bird:27228
Amazilia viridicauda	3,005	159901	http://arctos.database.museum/guid/MSB:Bird:27229
Amazilia viridicauda	2,953	168478	http://arctos.database.museum/guid/MSB:Bird:33259
Amazilia viridicauda	2,953	168480	http://arctos.database.museum/guid/MSB:Bird:33261
Amazilia viridicauda	2,900	168488	http://arctos.database.museum/guid/MSB:Bird:33269
Amazilia viridicauda	2,953	168493	http://arctos.database.museum/guid/MSB:Bird:33274
Coeligena coeligena	2,052	163658	http://arctos.database.museum/guid/MSB:Bird:31986
Coeligena coeligena	2,052	163741	http://arctos.database.museum/guid/MSB:Bird:32069
Coeligena coeligena	2,131	163914	http://arctos.database.museum/guid/MSB:Bird:32242
Coeligena coeligena	2,100	163915	http://arctos.database.museum/guid/MSB:Bird:32243
Coeligena coeligena	2,052	167517	http://arctos.database.museum/guid/MSB:Bird:32345
Coeligena coeligena	2,240	167534	http://arctos.database.museum/guid/MSB:Bird:32362
Coeligena coeligena	2,052	167823	http://arctos.database.museum/guid/MSB:Bird:32651
Coeligena violifer	2,798	163129	http://arctos.database.museum/guid/MSB:Bird:31564
Coeligena violifer	2,778	163210	http://arctos.database.museum/guid/MSB:Bird:31645
Coeligena violifer	2,810	163213	http://arctos.database.museum/guid/MSB:Bird:31648
Coeligena violifer	3,710	163485	http://arctos.database.museum/guid/MSB:Bird:31813
Coeligena violifer	2,858	168451	http://arctos.database.museum/guid/MSB:Bird:33232
Coeligena violifer	3,688	169121	http://arctos.database.museum/guid/MSB:Bird:33895
Coeligena violifer	3,688	169124	http://arctos.database.museum/guid/MSB:Bird:33898
Coeligena violifer	3,779	169232	http://arctos.database.museum/guid/MSB:Bird:34006
Oreotrochilus estella	4,363	169336	http://arctos.database.museum/guid/MSB:Bird:34110
Oreotrochilus estella	4,391	169357	http://arctos.database.museum/guid/MSB:Bird:34131
Oreotrochilus estella	4,512	169396	http://arctos.database.museum/guid/MSB:Bird:34170
Oreotrochilus melanogaster	3,840	163409	http://arctos.database.museum/guid/MSB:Bird:31737
Oreotrochilus melanogaster	3,750	163419	http://arctos.database.museum/guid/MSB:Bird:31747
Oreotrochilus melanogaster	3,974	168616	http://arctos.database.museum/guid/MSB:Bird:33397
Oreotrochilus melanogaster	4,150	168641	http://arctos.database.museum/guid/MSB:Bird:33422
Oreotrochilus melanogaster	4,088	168649	http://arctos.database.museum/guid/MSB:Bird:33430
Oreotrochilus melanogaster	4,082	168655	http://arctos.database.museum/guid/MSB:Bird:33436
Oreotrochilus melanogaster	4,140	168656	http://arctos.database.museum/guid/MSB:Bird:33437
Patagona gigas	3,360	159890	http://arctos.database.museum/guid/MSB:Bird:27221
Patagona gigas	3,967	163090	http://arctos.database.museum/guid/MSB:Bird:31526
Patagona gigas	3,967	163099	http://arctos.database.museum/guid/MSB:Bird:31535
Patagona gigas	3,973	163100	http://arctos.database.museum/guid/MSB:Bird:31536
Patagona gigas	3,973	163108	http://arctos.database.museum/guid/MSB:Bird:31544
Patagona gigas	3,750	163373	http://arctos.database.museum/guid/MSB:Bird:31701
Patagona gigas	3,750	163391	http://arctos.database.museum/guid/MSB:Bird:31719
Patagona gigas	4,082	168693	http://arctos.database.museum/guid/MSB:Bird:33474

Table S4. Cont.

Species	Elevation (m)	NK tissue no.	MSB catalog number and direct Weblink to specimen data
Phaethornis malaris	353	162160	http://arctos.database.museum/guid/MSB:Bird:27711
Phaethornis malaris	350	162199	http://arctos.database.museum/guid/MSB:Bird:27743
Phaethornis malaris	360	162253	http://arctos.database.museum/guid/MSB:Bird:31267
Phaethornis malaris	323	162297	http://arctos.database.museum/guid/MSB:Bird:31273
Phaethornis malaris	365	162333	http://arctos.database.museum/guid/MSB:Bird:27859
Phaethornis malaris	317	162362	http://arctos.database.museum/guid/MSB:Bird:27883

The listed Weblinks to the Museum of Southwestern Biology (MSB) online catalog provide detailed locality information and ancillary data for each of the 70 specimens.

Other Supporting Information Files

Dataset S1 (PDF)

Dataset S1. Phylogeny and trait data for comparative analyses. (A) The phylogeny that was used for the ancestral state estimates of elevation and β13- β83 genotype as depicted in Figure 4, in Newick format. Node labels are posterior probability estimates for each clade. Branch lengths are proportional to relative time. (B) The data used for comparative analyses of 63 hummingbird species, including the species' maximum elevation, minimum elevation, and the amino acids at positions β13 and β83.

A.

(apus_apus:42.5,((florisuga_mellivora:21.58251284,(eutoxeres_condamini:19.59179945,((threnetes_leucurus:7.593799152,glaucis_hirsutus:7.593799152)1.00:5.458735986,((phaethornis_syrmatophorus:7.040404114,(phaethornis_guy:4.536745179,phaethornis_malaris:4.536745179)0.87:2.503658935)1.00:0.7325615839,(phaethornis_hispidus:7.526412547,phaethornis_ruber:7.526412547)0.94:0.2465531508)1.00:5.27956944)1.00:6.539264308)1.00:1.990713397)1.00:0.8030054618,(((doryfera_ludovicae:12.78813896,(schistes_geoffroyi:11.77392866,colibri_coruscans:11.77392866)1.00:1.014210299)1.00:5.76138279,anthracothorax_nigricollis:18.54952174)1.00:1.5234818,(((((haplophaedia_aureliae:11.4814989,(eriocnemis_alinae:7.215116008,eriocnemis_luciani:7.215116008)1.00:4.266382893)1.00:2.348433693,((lafresnaya_lafresnayi:11.83844458,aglaeactis_castelnaudii:11.83844458)0.88:1.356892144,((((ensifera_ensifera:10.21230199,pterophanes_cyanopterus:10.21230199)1.00:1.625966458,(boissonneaua_matthewsii:10.11394209,ocreatus_underwoodii:10.11394209)1.00:1.724326357)0.97:0.5522489052,(clytolaema_rubricauda:9.184226467,((heliodoxa_imperatrix:4.600810376,heliodoxa_rubinoides:4.600810376)1.00:0.4850432233,heliodoxa_leadbeateri:5.085853599)1.00:4.098372868)0.99:3.206290882)1.00:0.4065088099,(coeligena_coeligena:9.655568467,(coeligena_torquata:6.102444883,(coeligena_violifer:4.772037487,(coeligena_iris:3.203338608,coeligena_lutetiae:3.203338609)1.00:1.568698878)1.00:1.330407396)1.00:3.553123583)1.00:3.141457693)0.73:0.3983105689)1.00:0.6345958663)1.00:1.671283968,(((lophornis_chalybeus:2.267283906,lophornis_delattrei:2.267283906)1.00:5.543762026,(discosura_longicauda:4.997402833,discosura_langsdorffi:4.997402834)1.00:2.813643099)1.00:6.403304237,(phlogophilus_harterti:13.21089492,((heliangelus_amethysticollis:3.530452247,(heliangelus_viola:3.261148903,heliangelus_micraster:3.261148903)0.99:0.269303344)1.00:8.587493192,((adelomyia_melanogenys:8.596382441,aglaiocercus_kingi:8.59638244)1.00:1.364615777,((oreotrochilus_estella:1.211047725,oreotrochilus_melanogaster:1.211047726)1.00:6.627644559,(polyonymus_caroli:7.495200005,((chalcostigma_herrani:5.130842394,(chalcostigma_stanleyi:4.811536371,(chalcostigma_ruficeps:4.571696761,chalcostigma_olivaceum:4.571696761)0.46:0.23983961)0.86:0.3193060232)1.00:0.9657565811,(metallura_phoebe:4.476686487,metallura_tyrianthina:4.476686487)1.00:1.619912488)1.00:1.398601031)0.94:0.3434922789)1.00:2.122305934)1.00:2.15694722)1.00:1.092949481)1.00:1.003455251)1.00:1.286866392)1.00:0.8534145773,(patagona_gigas:14.38065922,((eugenes_fulgens:11.524263,((calliphlox_amethystina:3.341953595,thaumastura_cora:3.341953595)1.00:1.683541112,selasphorus_platycercus:5.025494707)1.00:6.498768296)1.00:2.336386548,(chlorostilbon_aureoventris:12.43311726,(thalurania_furcata:11.33366768,(taphrospilus_hypostictus:8.855630206,((amazilia_amazilia:4.105048477,chrysuronia_oenone:4.105048477)1.00:1.242588118,(amazilia_lactea:2.914837093,(amazilia_chionogaster:1.796389023,amazilia_viridicauda:1.796389023)1.00:1.118448069)1.00:2.432799503)1.00:3.507993611)1.00:2.478037477)1.00:1.099449577)1.00:1.427532291)1.00:0.520009674)1.00:1.973971915)1.00:3.718372406)1.00:2.312514759)1.00:20.1144817);

B.

Species	Maximum elevation (m)	Minimum elevation (m)	β13	β83
Adelomyia melanogenys	2900	1000	Gly	Gly
Aglaeactis castelnaudii	4200	3100	Gly	Ser
Aglaiocercus kingi	2600	1300	Gly	Gly
Amazilia amazilia	1000	0	Gly	Gly
Amazilia chionogaster	2800	0	Gly	Ser
Amazilia lactea	900	0	Gly	Gly
Amazilia viridicauda	3100	1000	Gly	Ser

Anthracothorax nigricollis	1000	0	Gly	Gly
Apus apus	3300	0	Gly	Ser
Boissonneaua matthewsii	2700	1550	Gly	Ser
Calliphlox amethystina	1050	0	Gly	Gly
Chalcostigma herrani	3400	2700	Gly	Ser
Chalcostigma olivaceum	4500	3150	Ser	Ser
Chalcostigma ruficeps	3300	2250	Gly	Ser
Chalcostigma stanleyi	4400	3350	Ser	Ser
Chlorostilbon aureoventris	2500	0	Gly	Gly
Chrysuronia oenone	1650	0	Gly	Gly
Clytolaema rubricauda	2000	750	Gly	Gly
Coeligena coeligena	2200	1000	Gly	Gly
Coeligena iris	3500	1500	Gly	Ser
Coeligena lutetiae	3750	3000	Gly	Ser
Coeligena torquata	2800	1700	Gly	Gly
Coeligena violifer	3900	2500	Gly	Ser
Colibri coruscans	3600	1300	Gly	Ser
Discosura langsdorffi	800	0	Gly	Gly
Discosura longicauda	700	0	Gly	Gly
Doryfera ludovicae	2800	1200	Gly	Asn
Ensifera ensifera	3600	2200	Gly	Ser
Eriocnemis alinae	2800	2000	Gly	Ser
Eriocnemis luciani	3750	2600	Gly	Ser
Eugenes fulgens	3300	1300	Gly	Ser
Eutoxeres condamini	2750	0	Gly	Gly
Florisuga mellivora	900	0	Gly	Gly
Glaucis hirsutus	1100	0	Gly	Gly
Haplophaedia aureliae	2500	1400	Gly	Gly
Heliangelus amethysticollis	3300	1800	Gly	Gly
Heliangelus micraster	2900	2400	Gly	Gly
Heliangelus viola	3050	2150	Gly	Gly
Heliodoxa imperatrix	1800	900	Gly	Gly
Heliodoxa leadbeateri	2300	1050	Gly	Gly
Heliodoxa rubinoides	2650	1700	Gly	Gly
Lafresnaya lafresnayi	3350	2300	Gly	Ser
Lophornis chalybeus	600	0	Gly	Gly
Lophornis delattrei	2000	0	Gly	Gly
Metallura phoebe	4400	2500	Gly	Ser
Metallura tyrianthina	3500	2400	Gly	Ser
Ocreatus underwoodii	2500	1050	Gly	Ser
Oreotrochilus estella	4600	3400	Ser	Ser
Oreotrochilus melanogaster	4800	3500	Ser	Ser
Patagona gigas	4300	0	Ser	Ser

Phaethornis guy	2000	800	Gly	Gly
Phaethornis hispidus	500	0	Gly	Gly
Phaethornis malaris	1300	0	Gly	Gly
Phaethornis ruber	900	0	Gly	Gly
Phaethornis syrmatophorus	2400	1100	Gly	Gly
Phlogophilus harterti	1200	750	Gly	Ala
Polyonymus caroli	2800	1500	Gly	Ser
Pterophanes cyanopterus	3700	2600	Gly	Ser
Schistes geoffroyi	2250	1100	Gly	Gly
Selasphorus platycercus	3750	1900	Gly	Ser
Taphrospilus hypostictus	1350	750	Gly	Gly
Thalurania furcata	1700	0	Gly	Ser
Thaumastura cora	3000	0	Gly	Ser
Threnetes leucurus	1050	0	Gly	Gly